Agricultural Water Management 261 (2022) 107349

Contents lists available at ScienceDirect

Agricultural Water Management

journal homepage: www.elsevier.com/locate/agwat

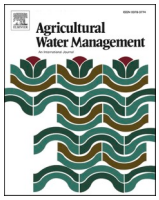

Assessing the grapevine crop water stress indicator over the flowering-veraison phase and the potential yield lose rate in important European wine regions

Chenyao Yang [a,*], Christoph Menz [b], Helder Fraga [a], Sergi Costafreda-Aumedes [c], Luisa Leolini [d], Maria Concepción Ramos [e], Daniel Molitor [f], Cornelis van Leeuwen [g], João A. Santos [a]

[a] Centre for the Research and Technology of Agro-Environmental and Biological Sciences (CITAB)/Inov4Agro - Institute for Innovation, Capacity Building and Sustainability of Agri-Food Production, University of Trás-os-Montes and Alto Douro(UTAD), 5000-581 Vila Real, Portugal
[b] Potsdam Institute for Climate Impact Research e. V. (PIK), Telegrafenberg A 31, 14473 Potsdam, Germany
[c] National Research Council of Italy, Institute of BioEconomy (CNR-IBE), 50019 Florence, Italy
[d] Department of Agriculture, Food, Environment and Forestry (DAGRI), University of Florence, Piazzale delle Cascine 18, 50144 Firenze, Italy
[e] Department of Environment and Soil Sciences, University of Lleida-AGROTECNIO-CERCA Center, Av.Rovira Roure 191, 25198 Lleida, Spain
[f] Luxembourg Institute of Science and Technology (LIST), 41 rue du Brill, 4422 Belvaux, Luxembourg
[g] EGFV, Univ. Bordeaux, Bordeaux Sciences Agro, INRAE, ISVV, F-33883 Villenave d'Ornon, France

ARTICLE INFO

Keywords:
Grapevine modelling
Drought stress
Yield gap
Phenology network
STICS
Regional crop modelling

ABSTRACT

In Europe, most of vineyards are managed under rainfed conditions, where water deficit has become increasingly an issue. The flowering-veraison phenophase represents an important period for vine response to water stress, which is known to depend on variety characteristics, soil and climate conditions. In this paper, we have carried out a retrospective analysis for important European wine regions over 1986–2015, with objectives to assess the mean Crop Water Stress Indicator (CWSI) during flowering-veraison phase, and potential Yield Lose Rate (YLR) due to seasonal cumulative water stress. Moreover, we also investigate if advanced flowering-veraison phase can lead to alleviated CWSI under recent-past conditions, thus contributing to reduced YLR. A process-based grapevine model is employed, which has been extensively calibrated for simulating both flowering and veraison stages using location-specific observations representing 10 different varieties. Subsequently, grid-based modelling is implemented with gridded climate and soil datasets and calibrated phenology parameters. The findings suggest wine regions with higher mean CWSI of flowering-veraison phase tend to have higher potential YLR. However, contrasting patterns are found between wine regions in France-Germany-Luxembourg and Italy-Portugal-Spain. The former tends to have slight-to-moderate drought conditions (CWSI<0.5) along with a negligible-to-moderate YLR (<30%), whereas the latter is found to have severe-to-extreme drought (CWSI>0.5) and substantial YLR (>40%). Wine regions prone to a high drought risk (CWSI>0.75) are also identified, which are concentrated in southern Mediterranean Europe. Advanced flowering-veraison phase over 1986–2015, could have benefited from more spring precipitation and cooler temperatures for wine regions of Italy-Portugal-Spain, leading to reduced mean CWSI and YLR. For those of France-Germany-Luxembourg, this can have reduced flowering-veraison precipitation, but prevalent reductions of YLR are also found, possibly due to shifted phase towards a cooler growing-season with reduced evaporative demands. Our study demonstrates flowering-verasion water deficit is critical for potential yield, which can have different impacts between Central and Southern European wine regions. This phase can be advanced under a warmer climate, thus having important implications for European rainfed vineyards. The overall outcome may provide new insights for appropriate viticultural management of seasonal water deficits under climate change.

* Corresponding author.
E-mail address: cyang@utad.pt (C. Yang).

https://doi.org/10.1016/j.agwat.2021.107349
Received 12 August 2021; Received in revised form 8 November 2021; Accepted 12 November 2021
Available online 24 November 2021

1. Introduction

Grapevine (*Vitis vinifera*) is a major fruit crop of economic importance worldwide. Europe is the world leader in wine production, which accounts for about 63% of world wine production in 2020 (OIV, 2021). Most of the winegrowing regions in Europe are currently cultivated under rainfed conditions, with only ~10% of vineyards irrigated, as a consequence of policy restriction (e.g. regulation rules in Denominations of Origin (DO)) and concerns for sustainable water use (Costa et al., 2016). For rainfed viticulture, water deficit stress has become increasingly an issue even in relatively cooler and wetter European countries, such as France, Germany and Luxembourg (Santos et al., 2020; van Leeuwen et al., 2019). This can be possibly attributed to the rising temperatures in the last decades, accompanied by more extreme weather events such as heatwaves (Fraga et al., 2020). Accordingly, the evapotranspiration from plant and soil has increased, which results in increasingly negative soil water balance (van Leeuwen et al., 2019). In southern Mediterranean countries, such as Italy, Portugal, Spain, vine growth is frequently exposed to drought stress, leading to reductions in yield and, if with severe water stress, impaired wine quality attributes (Costa et al., 2016; van Leeuwen et al., 2018). In these wine regions, water deficit combined with high temperatures in summer during the berry ripening period, can represent a major limiting factor for vineyard productivity (Chacón-Vozmediano et al., 2020; Costa et al., 2016). Moreover, water deficits can be further exacerbated under climate change in terms of frequency and intensity, which can be particularly pronounced in currently most vulnerable regions, e.g. southern Mediterranean regions (Costa et al., 2016; Giorgi and Lionello, 2008; Santos et al., 2020).

Mild or moderate water deficits generally favour the berry accumulation of sugar and some phenolics (e.g. anthocyanin), whereas severe water stresses can lead to significantly reduced berry quality (sugar, aroma) and grape yield (van Leeuwen et al., 2018, 2009). The effect of water availability varies with the variety. Limited water supply can increase skin phenolics (e.g. anthocyanins) which is crucial for the production of high-quality red grapes, whereas this may negatively affect the aromas of white grapes (van Leeuwen et al., 2019, 2018). However, the effects of water deficit also depend on its timing and duration (Gambetta et al., 2020). Before veraison, berries are hydraulically connected to vine and are sensitive to drought-induced shrivelling, but they are largely insensitive at/after veraison since berries become buffered from changes in vineś water status (Gambetta et al., 2020). Water shortage before veraison can have strong negative impacts on leaf growth, berry weight and final yield per vine (Chacón-Vozmediano et al., 2020; Gambetta et al., 2020; van Leeuwen et al., 2018; Wenter et al., 2018). One of the most important pre-veraison phenophase corresponds to the flowering-veraison phase, which proves to be an important period for berry weight and yield determinations (Chacón--Vozmediano et al., 2020; Gaudin et al., 2014; Ramos and Martínez-Casasnovas, 2014). For instance, Ramos and Martínez-Casasnovas (2014) found grape yield to be particularly sensitive to water availability of bloom-veraison period, during which a yield increase of about 46 kg/ha per mm water input is observed. Therefore, it is of importance to focus on how to increase water availability and mitigate possible water stress over this period, while not using irrigation when it is restricted. In southern Mediterranean countries, it is presumed an early occurrence of this phase can benefit from higher precipitations, as a considerable fraction of annual precipitation can occur between bud-break and flowering period (Ramos et al., 2020; Ramos and Martínez-Casasnovas, 2014). Besides, advanced flowering-veraison phase can reduce crop exposure to extreme high summer temperature that frequently exceeds 35 °C in these regions (Giorgi and Lionello, 2008; Yang et al., 2018). However, the magnitudes of these effects on alleviating water stress of flowering-veraison period are not quantified to our knowledge, especially over a large geographic area. Moreover, the potential impacts of such shifted phenophase in those relatively cooler and wetter European wine regions are yet to be well understood.

To determine the level of water deficit experienced by plants, measurements of leaf water potential at pre-dawn (Ψ_{pd}) and midday (Ψ_{mid}), and the stem water potentials (Ψ_{stem}), are often carried out, which are standard field methods to monitor vine water status (van Leeuwen et al., 2018, 2009). Although these are useful plant water stress indicators, they need frequent field measurements to obtain meaningful results, which are often laborious and costly. As an alternative, an empirical Crop Water Stress Indicator (CWSI), developed by Idso et al. (1981) and Jackson (1982), is also frequently applied to diagnose vine water status by relating the difference of canopy-air temperature to the air vapor pressure deficit of a non-water-stressed-baseline (Bellvert et al., 2015). CWSI can be conveniently estimated from remote-sensed thermal image data, which can allow us to accurately monitor vine water status throughout the growing season (Bellvert et al., 2015). However, to develop appropriate guidelines or agricultural policies for better management of seasonal water deficits, water stress indicators like CWSI need to be applied at the regional level to consider possible differences between vineyards in soil properties and climate conditions. For this purpose, several studies have applied biophysical models to simulate CWSI, for example, to monitor drought variability over the Koshi river basin in Central Asia (Wu et al., 2019) or for constructing the drought vulnerability curve for six main maize growing regions in China (Zhu et al., 2021).

Process-based crop models have proven to be useful tools to simulate the complex interactions among Genotypes, Management and Environment (G × M × E) and their impacts on desired outputs (e.g. water use and yield) (Coucheney et al., 2015; Rötter et al., 2018). The advantages of model-derived water stress indicators are being continuous over the season, which allow comparison between sites with different environmental conditions. By coupling with high-resolution gridded datasets, these models can be implemented at regional level to simulate crop water status and water stress conditions, taking into account genotype-dependent crop response to water deficits while integrating the effects of site-dependent climate variability and soil characteristics (Ceglar et al., 2019; Fraga et al., 2016; Zhu et al., 2021). Some of these models that have been successfully adapted to grapevine are UNIFI. GrapeML (Leolini et al., 2018a), PhenologyVv (Stock et al., 2007), UniPhen (Molitor et al., 2020) and STICS (Brisson et al., 2009; García de Cortázar-Atauri, 2006). In particular, Fraga et al. (2015) and Valdés-Gómez et al. (2009) have demonstrated a good agreement between water stress indices simulated by STICS and those measured in the field (Ψ_{pd} and Ψ_{mid}). STICS has also extensively shown its capacities in reliably simulating soil water content, plant water stress, phenology and yield for grapevine under various environmental conditions (Coucheney et al., 2015; Fraga et al., 2016, 2015; Valdés-Gómez et al., 2009).

For regional model applications, phenology parameters are the most common parameters to be calibrated/adjusted (Angulo et al., 2013; Ceglar et al., 2019), particularly for simulating phenology-dependent water stress. Besides, reliable phenology simulations can also contribute to improving estimations of potential yield that is closely related to the length of the growing season (van Ittersum et al., 2013). For winegrowers, it is not always beneficial to pursue higher yields, because they can compromise wine quality. But a reasonable production level should be safeguarded for wine growing estates to be economically sustainable. Therefore, it is of practical importance to understand and quantify to what extent the seasonal water stress can impose limitations on potentially attainable yields, especially to evaluate the role of a drought-sensitive period, i.e. flowering-veraison phase (Ramos et al., 2020; Ramos and Martínez-Casasnovas, 2014). Such yield-gap analysis is often carried out for annual field crops, like wheat and maize (van Ittersum et al., 2013). It is, however, rarely performed for grapevine, as overall more attention is given to quality attributes. Hence, our study may contribute to fill the gap in this regard.

In Europe, the leading five wine-producing countries are Italy (49.1 million hectoliter, i.e. mhl), France (46.6 mhl), Spain (40.7 mhl),

Germany (8.4 mhl) and Portugal (6.4 mhl), respectively (OIV, 2021). These countries together account for about 58% of world wine production in 2020, with a total exported wine worth ~19 billion euros (OIV, 2021). Adequate production of high-quality wines plays an important role in the local economy. Therefore, these countries were chosen in our analysis. Additionally, we have added Luxembourg that shares a wider wine region with Germany (the Moselle valley). Important wine regions are identified within these countries, accordingly. For these wine regions over a study period of 1986–2015, we aim to (i) assess vine drought stress conditions exclusively during the flowering-veraison phase, using CWSI that is constructed from model simulation outputs; (ii) assess the potential Yield Lose Rate (YLR) due to seasonal cumulative water stress (yield refers to mean cluster weight at harvest). The possible link between CWSI and YLR is also analyzed. Lastly, as a retrospective analysis, we also aim to (iii) investigate if shifted flowering-veraison phase can lead to both alleviated CWSI and YLR under recent-past conditions.

2. Data and methods

2.1. Workflow summary

An extensive site-based model calibration is performed using STICS model across studied wine regions, before being up scaled to regional level with grid-based simulations for CWSI and potential YLR over 1986–2015. Based on the setup, we also investigated potential impacts of early shifted flowering-veraison phase. A schematic overview of the workflow is presented in Fig. 1, which will be described in details in subsequent Sections.

2.2. Studied wine regions and selected sites in Europe

The major wine regions in the studied six European countries were identified (Fig. 2), in accordance with those in Fraga et al. (2020). Previous analysis revealed several wine regions in France, Germany and Luxembourg tended to be vulnerable to heatwave (Fraga et al., 2020). However, they are yet to be selected for a drought impact analysis, which are often connected with high temperature episodes. On the other hand, southern Mediterranean Europe such as Italy, Portugal and Spain, were already exposed to increasingly warmer and drier climate, accompanied by more frequent and longer weather extremes (Costa et al., 2016). Mediterranean region was projected to be one of the meteorological drought "Hot Spots" (Giorgi and Lionello, 2008).

Across these wine regions, 38 sites were selected (Fig. 2) where the flowering (BBCH65) and veraison data (BBCH81) were obtained for 10 different grapevine varieties (representing locally dominant varieties) (Table S1). The data was mainly collected within the framework of the Clim4Vitis project (https://clim4vitis.eu/) from vineyard based observations, but also complemented by data from the Pan European Phenology project (PEP725) (Templ et al., 2018) and from the Italian Phenological Network (IPHEN) (Mariani et al., 2013). However, it shall be emphasized that PEP725 data lacked specific variety information for our selected sites, while IPHEN data generally covered short periods. Observed data was only used for calibration when fulfilled the following criteria: (1) data was measured within the study period (1986–2015); and (2) flowering and veraison stages were recorded in the same year (except sites with only flowering or veraison data). Detailed information on the site coordinates and names, related varieties, data length and source, were summarized in Table S1.

2.3. STICS-grapevine modules

This section presented STICS-grapevine modules (*v*9.2) that were most relevant in this study, while a more comprehensive presentation of the model structure and formalisms can be found in several other studies (Brisson et al., 2003, 2009, García de Cortázar-Atauri et al., 2009a,b; García de Cortázar-Atauri, 2006).

2.3.1. Phenology module

The phenophase between dormancy onset and budbreak was simulated using the BRIN model, which successively calculated the period from dormancy onset to dormancy break, and from dormancy break to budbreak (García de Cortázar-Atauri et al., 2009a). The dormancy period calculation was based on Bidabe's cold action model (Bidabe,

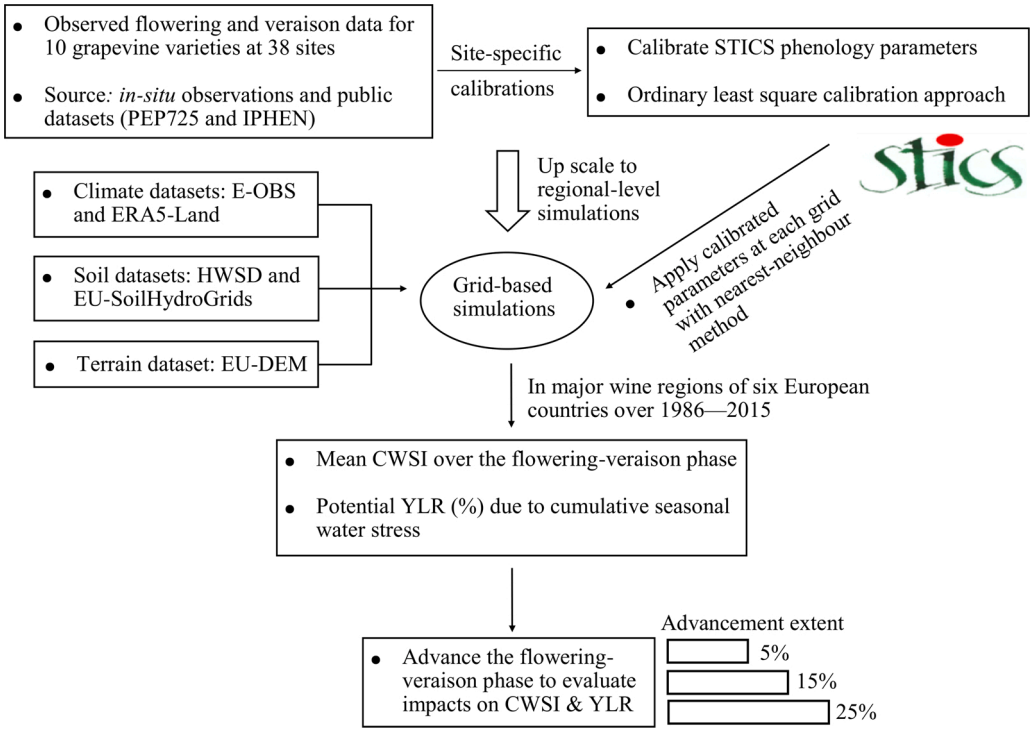

Fig. 1. The schematic workflow of the analysis.

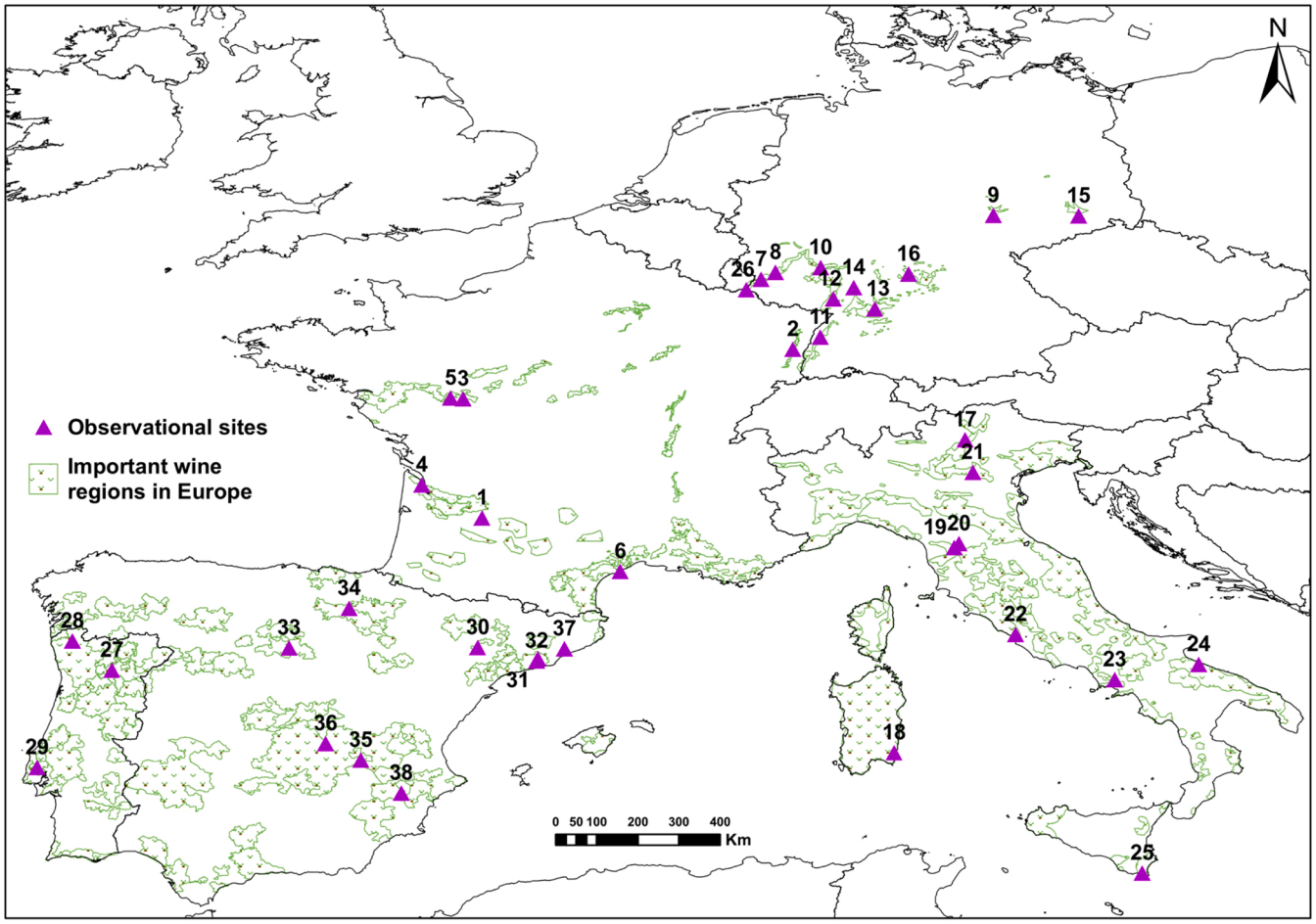

Fig. 2. Study sites and important wine regions across six different European countries. The site ID is denoted, which is consistent with those indicated in the Table S1.

1965), taking into account the genotype-dependent chilling requirement expressed as chilling units or effective Dormancy Days (*DD*). The post-dormancy period (after dormancy break) was calculated based on Richardson's chilling hour units (Richardson et al., 1974), with cardinal temperatures defined to limit the function of a linear response. A critical sum of growing degree hours (*PD*: post-dormancy thermal requirement) was considered and assumed to be genotype-dependent. The subsequent stages such as flowering, veraison and fruit maturity, were all simulated using the classic Growing Degree Day (GDD, Celsius degree-day) model with a 10 °C base temperature (Brisson et al., 2009). The flowering stage was mainly controlled by two parameters, which defined budbreak to fruit setting and flowering to fruit setting period, respectively. The former one was generally a sensitive parameter with substantial influence on other simulation outputs (e.g. LAI, biomass and yield), whereas the latter one was only built for additional adjustment of flowering stage without any effects on the other processes (Brisson et al., 2009). Thus, we only chose to calibrate the GDD requirement between the budbreak and fruit setting onset, which was denoted as *FL*. For the veraison onset, the parameter for GDD requirement between the end of juvenile phase and veraison onset was chosen for calibration, defined as *VR*. These phenology parameters are all genotype-dependent.

2.3.2. Water use module

Soil water balance simulations represented an essential component of soil-crop system modeling. The resulting simulated maximum (ET_{max}) and actual evapotranspiration (*ET*) largely determine the soil water content and the crop water stress conditions, which in turn affects the potential canopy growth, biomass accumulation and yield at harvest. The ET_{max} can be divided into maximum soil evaporation (E_{max}) and crop transpiration (T_{max}). For grapevine, the E_{max} was estimated by available energy in the soil surface, following the energy balance approach (Brisson et al., 2009) (cf. Supplementary Material for details). The actual soil evaporation (*E*) was calculated by a semi-empirical model developed by Brisson and Perrier (1991): soil evaporation is maximum (E_{max}) until reaching a cumulative threshold (estimated by particle size distribution). Then *E* is calculated considering the soil type, weather influence and most importantly the actual soil water availability (Brisson et al., 2009).

T_{max} represents the crop water requirement, which was calculated using the Shuttleworth and Wallace (S-W) model (Shuttleworth and Wallace, 1985). S-W is a resistance model that characterizes the soil-plant-atmosphere system with a resistance network, which proved to be effective in explaining the canopy energy budget (Brisson et al., 1998). The advantage of using the S-W model consists in its ability to consider the influence of soil evaporation on T_{max}, whereas this is absent in other approaches (e.g. dual crop coefficient) (Allen et al., 1998). However, S-W is a complex model holding many parameters and assumptions, while a variety of input data on meteorology and crop characteristics (e.g. canopy height) is required (Brisson et al., 1998) (cf. Supplementary Material for detailed T_{max} calculations). The actual transpiration (*T*) is calculated based on the available soil water content in the root zone. Crop transpiration is at the maximum rate (T_{max}) unless the available soil water content is below a certain threshold. Such threshold was calculated at a daily time step, depending on the root density, a plant stomatal function and T_{max} (Brisson et al., 2009). The ratio T/T_{max} was computed as the crop water stress index, which was shown to be closely correlated with measured Ψ_{pd} and Ψ_{mid}, with a variety-dependent R^2 up to 0.89 and 0.94 respectively (Fraga et al.,

2015; Valdés-Gómez et al., 2009).

2.3.3. Yield module

Yield formation was essentially a process of dry matter allocation to fruits during the fruit-setting to maturity period. A boxcar train technique was applied to account for the asynchronous nature of berry maturation with the concept of fruit-age class (number of artificially imposed berry growth compartments) (Goudriaan and van Roermund, 1993). It attempted to mimic the physiological changes occurring over the berry ripening process. For each compartment, the berry growth (a dry-matter allocation coefficient) was differently calculated, depending on the number of setting berries, potential berry growth rate (cell division and expansion), and possibly any abiotic stress effects (García de Cortázar-Atauri et al., 2009b).

2.4. Simulation setup

2.4.1. Automatic model calibrations at selected 38 sites

The purpose of the phenology calibration (partial calibration) was to partly account for (sampling) the considerable spatial variabilities of genotypes used in these wine regions. For each study site (Fig. 2 and Table S1), the four phenology parameters explained in Section 2.3.1, were calibrated. A range was predefined for each of these parameters: *DD* (40−205), *PD* (6000–11500), *FL* (230–560), and *VR* (600–1700). These ranges generally covered a large genotypic variability (García de Cortázar-Atauri, 2006), which were evenly sampled with 11 intervals per parameter, resulting in a total of ~20,000 parameter combinations tested per site. Parameter-induced variations represented a major source of uncertainties in crop model simulations, while estimations of best-fit parameters rely on a clearly outlined calibration approach (Seidel et al., 2018; Wallach et al., 2011). We estimated parameter values by minimizing the sum of mean squared error (MSE) between observations and simulations over the two successive stages, following the ordinary least square approach (Wallach et al., 2011). Previous analysis revealed that minimizing the sum of MSE was an appropriate goodness-of-fit criterion, particularly when there were multiple measurements over time in the same plot (containing prediction error correlation and heteroscedasticity) (Wallach et al., 2011). However, when only flowering or veraison data was available (total 8 sites), the MSE was minimized for a single-stage accordingly. Following the model calibration, the goodness-of-fit between observations and simulations with estimated parameters, were evaluated using Mean Biased Errors (MBE), Mean Absolute Errors (MAE), Root Mean Squared Errors (RMSE) and Pearson correlation coefficient (*r*). Refer to Yang et al. (2021) for more details on the overall calibration approach. The calibrated parameters, shown in Fig. S1, can generally well reproduce the inter-annual variability of observed data with negligible mean bias (Fig. S2–S6). Detailed description of overall calibration results (including the goodness-of-fit between observations and simulations for each site) was presented in the supplementary material.

2.4.2. Input data for grid-based simulations

Grid-based simulations were feed with inputs from estimated phenology parameters from the closest (measured by Euclidean distance) calibration site, and from gridded climate, soil and terrain datasets (Fig. 1). The required daily surface temperature (°C) and precipitation sum (mm) were directly obtained from the recent release of the E-OBS dataset (v22.0e) at an enhanced resolution of 0.1°× 0.1° (Cornes et al., 2018). Mean seasonal (April–September) temperature (°C) and precipitation sum (mm) were calculated over 1986–2015. Besides, we also calculated maximum consecutive number of hot days (CHD: consecutive days with daily maximum temperature>25 °C) and of dry days (CDD: consecutive days with daily total precipitation<1 mm), to characterize the duration of extreme events over 1986–2015. Daily surface solar radiation (MJ m^{-2} day^{-1}), wind speed (m s^{-1}) and actual vapor pressure (hPa), were obtained and processed from ERA5-Land hourly reanalysis data (0.1°×0.1°) (Muñoz Sabater, 2019). The hourly 10-m wind speed was firstly calculated from respective zonal and meridional wind components, before being adjusted to the standard 2-m height following logarithmic profile (Allen et al., 1998). Daily mean vapor pressure was estimated from the dew-point temperature at daily minimum and maximum, with the exponential function (Allen et al., 1998).

For soil inputs, some important soil properties such as soil texture, particle size distribution, pH, bulk density and surface dry albedo, were retrieved from the Harmonized World Soil Database (HWSD, v1.2) at ~1 km resolution (FAO/IIASA/ISRIC/ISSCAS/JRC, 2012). Soil hydraulic properties (e.g. field capacity and wilting point), were derived from EU-SoilHydroGrids 1 km (v1.0), which provided European-wide estimates at seven standard soil depths (up to 2 m) (Tóth et al., 2017). To account for complex terrain conditions, the European Digital Elevation Model (EU-DEM, v1.1) at 25 m grid resolution, was employed to supply surface slope information. More detailed information on how gridded soil datasets were assimilated into STICS is available in Yang et al. (2020). By overlaying the climatic grids, soil and terrain maps, the simulation unit was determined at a regular grid of 0.1°× 0.1° resolution, taking into account the trade-off between accuracy in resolving spatial gradients and computation workloads (avoid excessive and repetitive soil information appearing within a given climatic grid). It was noteworthy the gridded data was also used for aforementioned site-based calibrations.

2.4.3. Assessing the CWSI and YLR (%) over 1986–2015

Mean CWSI of the flowering-veraison phase (hereafter CWSI) was computed at each grid point for each year over 1986–2015. The CWSI was computed according to Zhu et al. (2021):

$$\mathrm{CWSI} = 1 - \frac{ET}{ET_{max}} \tag{1}$$

where ET and ET_{max} were daily model outputs with detailed calculation procedures explained in Section 2.3.2. It integrated the effect of climate, soil and crop characteristics, which has been widely applied for drought monitoring and assessment (Wu et al., 2019; Zhu et al., 2021). According to Wu et al. (2019), CWSI can be divided into four categories: 0–0.25 as slight drought, 0.25–0.5 as moderate drought, 0.5–0.75 as severe drought and 0.75–1 as extreme drought (Wu et al., 2019). Similar to Zhu et al. (2021), CWSI was calculated as the mean instead of sum over a target phase, with the advantages to preserve its physical meanings and allow comparison of drought intensities among regions.

The potential YLR(%) was also simulated for each grid over 1986–2015, which, in accordance with Zhu et al. (2021), was computed as follow:

$$\mathrm{YLR}(\%) = \left(1 - \frac{Y_{stress}}{Y_{potential}}\right) \times 100\% \tag{2}$$

where Y_{stress} and $Y_{potential}$ were the potential cluster weight (g) at harvest simulated with and without water stress, respectively. To reduce uncertainties of spatial simulations associated with heterogeneous vineyard managements, we focused only on mean cluster weight (g) at harvest (hereafter referred to as yield). The advantage was to avoid the need to specify the other two yield components: local planting density (vines/ha) and mean harvestable cluster numbers per vine (dependent on the variety, training system and viticulture practices). $Y_{potential}$ represented potentially attainable yield in absence of any abiotic and biotic stresses, together with optimum farming practices (van Ittersum et al., 2013). It is only affected by seasonal temperature, radiation, CO_2 level and crop genetic traits (e.g. potential fruit size/number). For rainfed crop, $Y_{potential}$ can also be interpreted as yield under full watered conditions while keeping the other field managements optimal. Y_{stress} represented water-limited potential yield, in which $Y_{potential}$ is additionally limited by seasonal water supply (van Ittersum et al., 2013). Therefore,

YLR aimed to quantify the effects of seasonal cumulative water stress on potential yield.

For impact assessment, on top of average effects over a time-series, particular attentions should be paid to extreme events (e.g. drought, heatwave) that can cause significant yield reductions. Therefore, possible extreme events for CWSI and YLR were assessed over 1986–2015, based on the fixed exceeding probability of 5- and 20-year return periods respectively. The return period calculation was based on the empirical cumulative distribution function fitted for each grid point over 1986–2015.

2.4.4. Evaluate the effects of shifting the phenophase (flowering-veraison)

Water stress during the flowering-veraison phase can represent a major contribution to total water stress effects (Ramos et al., 2020; Ramos and Martínez-Casasnovas, 2014). Therefore, it was of interest to examine if potential YLR can be reduced by alleviating the CWSI during this period. Specifically, we have modified the calibrated phenology parameters for each grid point, at which the required thermal demand (GDD) for flowering (*FL*) and veraison stage (*VR*) was simultaneously reduced by 5%, 15%, 25% respectively. Accordingly, the phenophase between two stages was shifted earlier where the resulting advancements in days were calculated. In vineyards, this can be achieved by introducing different grapevine varieties (15–25% shift) or different clones of the same variety (5% shift) to preserve local wine typicity (Parker et al., 2013; van Leeuwen et al., 2019). The difference for CWSI and YLR without and with the shifted phenophase was calculated respectively. Note for YLR, only variations on Y_{stress} were considered while $Y_{potential}$ remained constant (equation 2). The Mann-Whitney rank test (Mann and Whitney, 1947) was performed to assess if their distributions over 1986–2015 became different (statistical significance at $p <= 0.05$) after the shifted phenophase. Consequently, we estimated potential YLR as a function of mean CWSI over the flowering-veraison phase, to evaluate respective drought vulnerability.

3. Results and discussion

3.1. Meteorological characteristics in major wine regions

Most of the studied wine regions were well confined within suitable viticulture regions worldwide defined by the isotherms of the mean seasonal temperature of 12–24 °C (Schultz and Jones, 2010). However, the mean seasonal (April–September) temperature over 1986–2015 is markedly higher (~16–22 °C) in I-P-S countries, whereas it is lower (~12–18 °C) in F-G-L countries (Fig. 3a). Some wine regions in southern Spain (e.g. Extremadura) have a high seasonal temperature (>22 °C) close to the upper boundary of optimal range (Fig. 3a). For mean seasonal total precipitation (mm) over 1986–2015, there are considerable spatial heterogeneities (Fig. 3b). Precipitation > 300 mm is generally observed in F-G-L countries, whereas dry areas with precipitation < 150 mm are identified in regions of I-P-S countries (e.g. Alentejo, Extremadura, La Mancha, Puglia, Sicily) (Fig. 3**b**). However, precipitation between 300 and 600 mm is also found in areas in northwest Portugal (e.g. Minho) and northern Italy (e.g. Friuli Venezia Giulia) (Fig. 3**b**). For the identified dry regions, such as La Mancha DO, impacts of severe water stress are already pronounced, particularly during summer (Chacón-Vozmediano et al., 2020). For the calculated CHD and CDD, they are generally < 60 days for most of the wine regions in F-G-L countries (Fig. 3**c–d**). In contrast, for southern Mediterranean countries (I-P-S), CHD and CDD are mostly 60–120 and 90–150 days, respectively (Fig. 3c–d). In central and southern Spain, CHD can last for more than 4

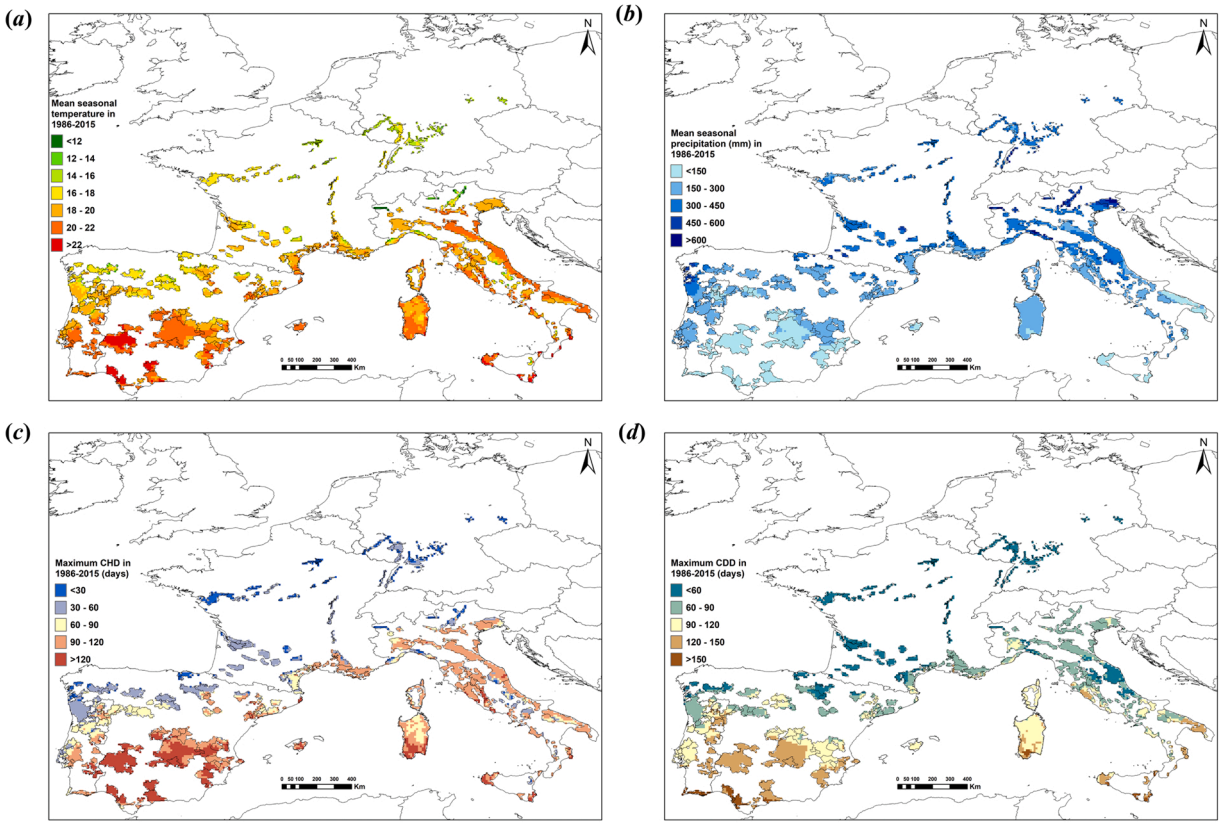

Fig. 3. Characterization of climate conditions for important wine regions across six European countries over the study period (1986—2015) for the (***a***) mean seasonal (April—September) temperature (°C); (***b***) mean seasonal (April—September) total precipitation (mm); (***c***) maximum consecutive hot days (CHD) over the period where CHD are counted when daily maximum temperature > 25 °C; (***d***) maximum consecutive dry days (CDD) over the period where CDD are counted when daily precipitation < 1 mm.

months (Fig. 3**c**). It is thus corroborating that regions with averagely warmer and drier climates are more prone to prolonged extreme events over 1986–2015 (Fig. 3). Extreme weather events, such as heatwaves and dry spells, are not only important in terms of frequency and intensity, but also the continuousness that was shown to pose substantial threats to vineyards productivity across Europe (Fraga et al., 2020).

3.2. Mean CWSI of the flowering-veraison phase (CWSI)

For mean CWSI (CWSI for brevity), the median and possible extreme values (return-period calculations) are assessed over 1986–2015 (Fig. 4a–c). The median values over 1986–2015, generally vary from 0 to 0.5 (slight to moderate drought) in F-G-L countries (except some areas in southern France), to 0.5–1.0 (severe to extreme drought) in I-P-S countries (except some areas in northern Italy and northwest Portugal) (Fig. 4a). Rare CWSI events with 5- and 20-year return periods (20% and 5% chance of being exceeded in magnitude for any given year), primarily correspond to widespread severe drought (>0.5) and severe-to-extreme drought (>0.625) respectively (Fig. 4b–c). Yet, higher CWSI values are mostly found in I-P-S countries, where extreme CWSI (>0.75) is detected for most of the Iberian Peninsula (Fig. 4b–c). The associated zonal average of each wine region shows an increase of drought severity from north to south within each country (except for G-L) (Fig. S7). Overall, wine regions prone to a high drought risk of the flowering-veraison phase (CWSI>0.75) (hereafter drought-prone regions), are identified as those in Iberian Peninsula (except north-western Portugal), southern areas in France (Languedoc, Provence, Rhone) and Italy (Apulia, Sardinia, Sicily) (Fig. 4a–c) (Fig. S7). Among these regions,

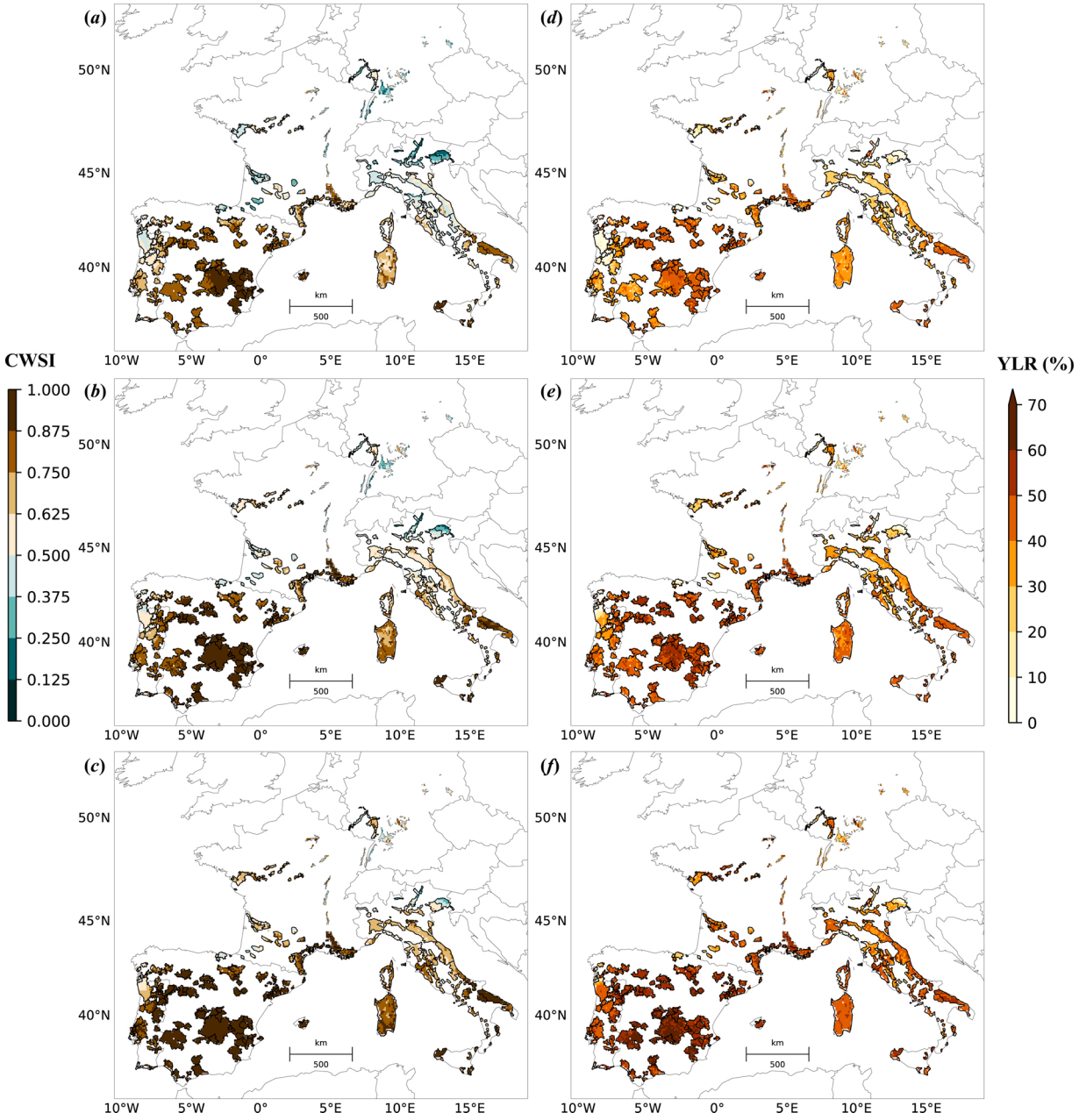

Fig. 4. The simulated (***a—c***) mean crop water stress indicator (CWSI) of the flowering-veraison phase (left panels) and (***d—f***) the potential yield loss rate (YLR, %) due to seasonal cumulative water stress (right panels) in studied wine regions over 1986—2015. The calculations for each grid point correspond to (***a, d***): the median values and (***b, e***): values at the fixed exceedance probability with 5-year return period and (***c, f***) with 20-year return period. The return period calculation is based on the empirical cumulative distribution function over 1986—2015.

CWSI is the highest (>0.875) with extreme drought for wine regions in central and south-eastern Spain (e.g. Extremadura, La Mancha, Manchuela) (Fig. 4a–c) (Fig. S7).

These results can be mostly associated with the spatial pattern of precipitation during the flowering-veraison phase, which is particularly limited for those drought-prone regions with median values < 50 mm accompanied by strong inter-annual variability (CV>80%) (Fig. S8). Notably, these regions also have high CDD and CHD (Fig. 3c–d), which implies the absence of precipitation can frequently occur over the flowering-veraison phase, during which *ET* is close to 0, i.e. CWSI close to 1 in most wine regions of Spain (Fig. S7). For rainfed Mediterranean viticulture, most of the berry growth and ripening periods are frequently exposed to conditions of high temperature and soil water deficits, which are particularly pronounced for Iberian Peninsula (Chacón-Vozmediano et al., 2020; Costa et al., 2016). In particular, Ramos and Martínez-Casasnovas (2014) highlighted water deficit was consistently more severe during bloom-veraison period than in other growing phase for Cabernet Sauvignon in Penedès DO (Spain) over 1998–2012. The overall spatial pattern of CWSI is consistent with that in Fraga et al. (2016), which simulated water stress index from fruit-setting onset to maturity, concluding that stronger water stress was mainly found in Iberian Peninsula and Italy. Compared to the previous work, we have additionally tried to consider (sample) spatial variations of local varieties in CWSI simulations, as well as incorporating recent gridded datasets with a finer spatial resolution (0.1°×0.1°). However, it shall be cautioned that CWSI calculations rely on the S-W resistive model for estimating evapotranspiration, which might require additional verifications. But available lysimeter measurements with quality records are very scarce across these wine regions. On the other hand, since water stress can be associated with excessively high temperatures, a previous analysis revealed most of these drought-prone regions are also frequently exposed to detrimental impacts of heatwaves (Fraga et al., 2020).

3.3. Potential YLR due to seasonal water stress (YLR)

The quantified median YLR over 1986–2015 shows a similar spatial pattern as that of CWSI, with higher YLR in I-P-S countries than in F-G-L countries (Fig. 4**d**). The median YLR mainly varies at about 20–45% in Italy, 10–40% in Portugal and 30–50% in Spain to about 20–40% in France, 10–30% in Germany and negligible (<5%) in Luxembourg (Fig. 4**d** and Fig. S9). Rare YLR events with a 5-year return period, mainly correspond to prevalent YLR at about 30–50% in I-P-S (some areas>50% in Spain) and 20–40% in F-G countries (some areas>40% in southern France) (Fig. 4**e** and Fig. S9). With a 20-year return period, YLR mostly amounts to around or greater than 50% in I-P-S (some areas>60% in Spain), whereas it is about 40–50% for most of France (some southern areas >50%) and generally < 40% for Germany (Fig. 4**f**) (Fig. S9). Potential YLR is generally not important for the studied wine region in Luxembourg, with an extreme YLR of only around 20% (Fig. S9). For the aforementioned drought-prone regions, the potential YLR is essentially around 30–60% (close to 60% for rare events) (Fig. 4**d–f** and Fig. S9).

These results reveal wine regions with stronger CWSI during flowering-veraison phase tend to have higher potential YLR, particularly for the identified drought-prone regions (Fig. 4). Compared to observations, the quantified median YLR is comparable to a recent meta-analysis, which reported approximately 7–45% reductions in berry weight of Cabernet Sauvignon, Merlot and Tempranillo (involved in our analysis) under moderate-to-severe water deficits ($-1.4 < \Psi_{stem} < -0.9$) as compared to non-stressed conditions (Gambetta et al., 2020). In a Mediterranean region (northern Italy), Wenter et al. (2018) showed about 46–51% reductions in berry weight of Sauvignon blanc between rainfed and full-irrigated conditions. However, it shall be emphasized though grid-based simulations already assimilate phenology data, the growth parameters, such as potential leaf growth and photosynthesis capacity, are not adjusted locally to reflect yield response to water deficits at variety-level. Thus, some uncertainties exist in the simulated magnitudes of potential YLR.

3.4. Effects of shifting the flowering-veraison phase over 1986–2015

3.4.1. Advanced flowering and veraison stages

The grid-based phenology simulations, driven by sited-based observations of local varieties, show the mean flowering and veraison DOY are mostly 135–180 and 180–240 respectively (Fig. S10). These ranges are in line with Fraga et al. (2016), who reported that flowering generally occurred from the 2nd week of May until the end of June while veraison occurred from the end of June to the end of August across major European wine regions. In response to 5%, 15%, 25% advanced phenophase at each grid point, median flowering DOY is respectively advanced by < 5 days, 5–10 days, 5–15 days throughout, while median veraison DOY is advanced by < 5 days, 5–20 days, 10–30 days (Fig. S10). The simulated magnitudes of these advancements can be achieved for example by introducing different cultivars. As existing difference among cultivars already shows 16 and 31 days (between earliest and latest) for flowering and veraison stage respectively (Parker et al., 2013). Similarly, van Leeuwen et al. (2019) also found the average veraison date can span up to 34 days among 52 grapevine varieties. On the other hand, under climate change with rising temperature, all phenology stages are projected to occur earlier for both early and late varieties (Leolini et al., 2018b; Ramos, 2017). The flowering-veraison phase is expected to be shortened, which can have important implications on CWSI: increased evaporative demand under a warmer climate but with a shorter time-window for water stress. Consequently, advanced phenology has important repercussions on wine quality. Because the grape composition can be unbalanced (e.g. between sugar and polyphenols) if grape achieves full ripeness in the warmest part of the season (July–August) (Ramos and Martinez de Toda, 2020; van Leeuwen et al., 2019; van Leeuwen and Seguin, 2006). Besides, advanced phenology also implies a shorter growing phase with early maturity, which can lead to changes in the sensation attribute, e.g. more astringent wine due to inadequate ripeness (García-Estévez et al., 2017). Minimal pruning or semi-minimal-pruned hedge can help delay the fruit maturity with improved fruit quality, e.g. with increased anthocyanin concentration or higher degree of organic acids (Schäfer et al., 2021; Zheng et al., 2017). However, delayed fruit maturity might still be exposed to an increased frequency of high-temperature episodes that could be extended from August to September under climate warming (with increased incidence of fruit sunburns), particularly in those southern Mediterranean regions.

3.4.2. Variations of mean CWSI in flowering-veraison period

For median precipitation of the flowering-veraison phase over 1986–2015, advanced phenology seems to result in an overall decrease (<25 mm) for F-G-L (except some areas in southern France), but a small increase (<12.5 mm) for I-P-S (except some areas in northern Italy and central Spain) countries respectively (Fig. S8). These small median changes indeed result from strong inter-annual variability of changes in flowering-veraison precipitation with shifted phenophase (Fig. S11). Significant median changes of precipitation are only evident with 25% shifted phenophase, primarily in Germany (significant less) and southern Spain (significant more) (Fig. S8). Across all wine regions, it can have widespread decreases by up to 75 mm (5th percentile) for a given year, while having prevalent increases by up to 125 mm (95th percentile) in another year (Fig. S11). The 90% uncertainty range (difference between 5th and 95th percentile) over 1986–2015 for each grid point generally indicates a higher chance of precipitation gains (–25 to 100 mm) in the drought-prone regions, as compared to a range of –75 to 75 mm in F-G-L countries (Fig. S11). The results suggest despite remarkably larger inter-annual variability of flowering-veraison precipitation in I-P-S (60–160% CV) than in F-G-L (<60% CV) countries (shown in Fig. S8), shifted phenophase still favours more precipitation in

the former case. This is mainly because precipitation is concentrated in autumn-winter and spring seasons for southern Mediterranean Europe (Costa et al., 2016; Giorgi and Lionello, 2008), where a significant fraction of annual rainfall can occur before grapevine flowering stage (Ramos and Martínez-Casasnovas, 2014). However, this might not be effective for F-G-L countries with a relatively even seasonal precipitation distribution, although increased precipitation during flowering-veraison phase is not as important as that in I-P-S countries. With respect to the effects of shifted phenophase on CWSI, there are also considerable uncertainties across all wine regions (Fig. S12), which can be mainly linking to the marked inter-annual variability of flowering-veraison precipitation (Fig. S8 and Fig. S11). However, CWSI shows a tendency of reductions by up to 0.2 for I-P-S countries (but mainly with 25% shifted phenophase), while being more uncertain –0.2 to 0.2 (90% uncertainty range) in F-G-L countries (Fig. S12). As a result of inter-annual variability, median variations for CWSI over 1986–2015, primarily range from –0.05 to 0.05 across all wine regions (Fig. 5). Slight reductions (alleviations) of CWSI are detected throughout I-P-S countries and southern France, in which statistical significances ($p < 0.05$) are only discovered under 25% shifted phenophase and mainly in those

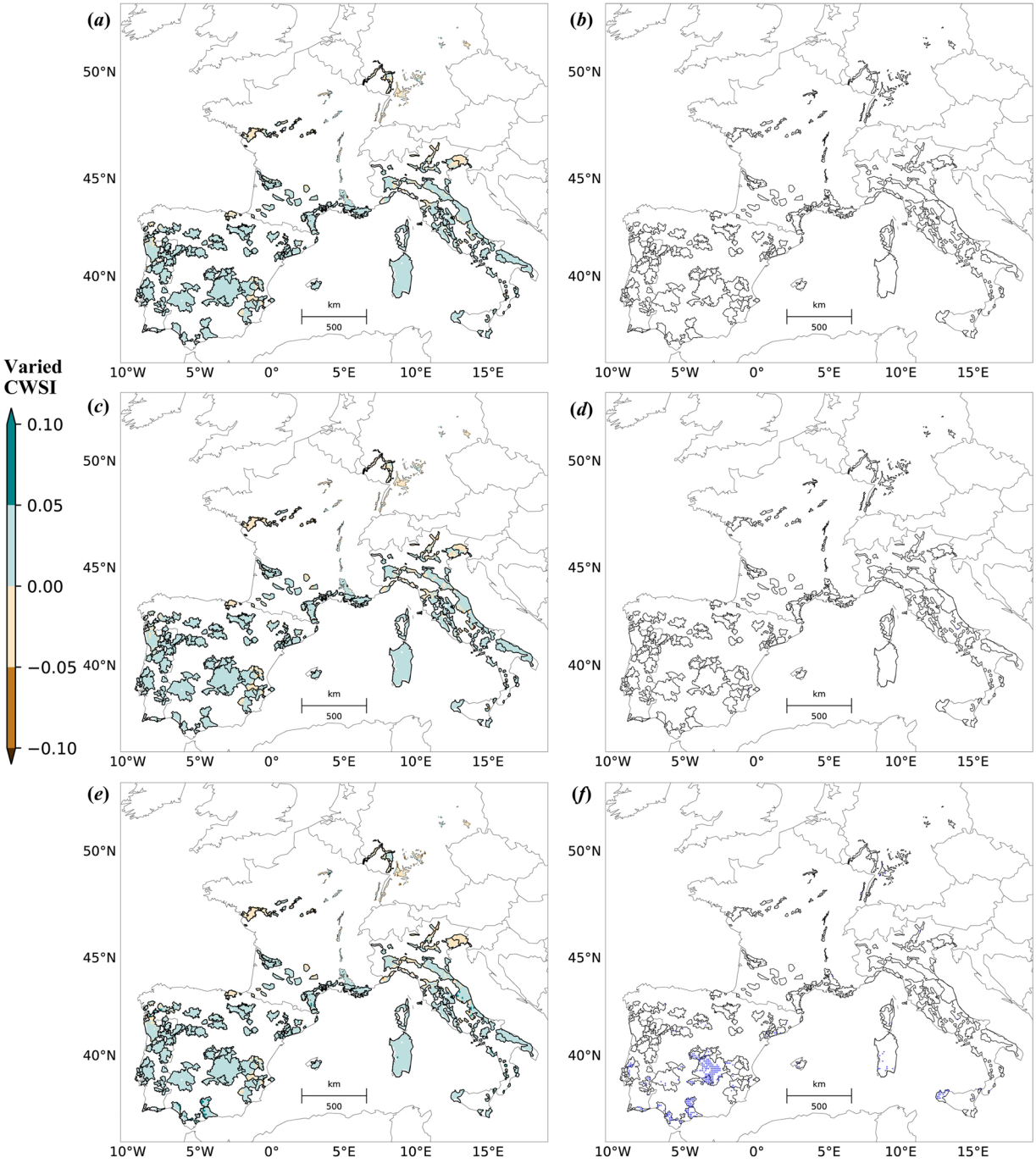

Fig. 5. The median of the variations of the mean crop water stress indicator (CWSI) between the flowering and veraison stage by shifting the flowering-veraison phase (***a, b***): 5% earlier, (***c, d***): 15% earlier and (***e, f***): 25% earlier. In the right panels, the Mann-Whitney rank test is performed to check if median CWSI over 1986—2015 becomes significantly different at $p <= 0.05$ (see Section 2.4.4). Significant grids are marked with blue plus symbols, whereas grids without colours indicate no significance (empty areas). For each grid point, the variations of CWSI over 1986—2015 are calculated as the difference without and with the shifted phenophase (positive values for reductions on CWSI).

drought-prone regions (Fig. 5**e–f**). In contrast, slight increase in median CWSI is found for F-G-L countries, but without statistical significance (Fig. 5). It also should be emphasized that shifted phenophase could have led to cooler temperatures with reduced evaporative demand (ET_{max}) in wine regions of I-P-S, thus contributing to reduced CWSI (Chacón-Vozmediano et al., 2020; Costa et al., 2016). Such effects can also be expected for those of F-G-L, although the magnitude of cooling can be smaller than those in I-P-S (not shown).

For the drought-prone regions in I-P-S countries, changes in the water deficits during the flowering-veraison phase could especially affect the grape quality. For not irrigated vines, rainfall is the unique water input and the time in which it fells can affect the acidity and phenolic composition, particularly in the context of global warming. For instance, in some of the Spanish wine regions, where most of vines are cultivated with red varieties and early phenology and without irrigation, lower water deficits in the flowering-veraison period favour an increase in acidity (Ramos et al., 2015), while an increase in water deficits in this period favours an increase in anthocyanins (Ramos and Martínez de Toda, 2020). These effects, depending on how the water deficits can vary, could potentially balance the decreases on grape quality

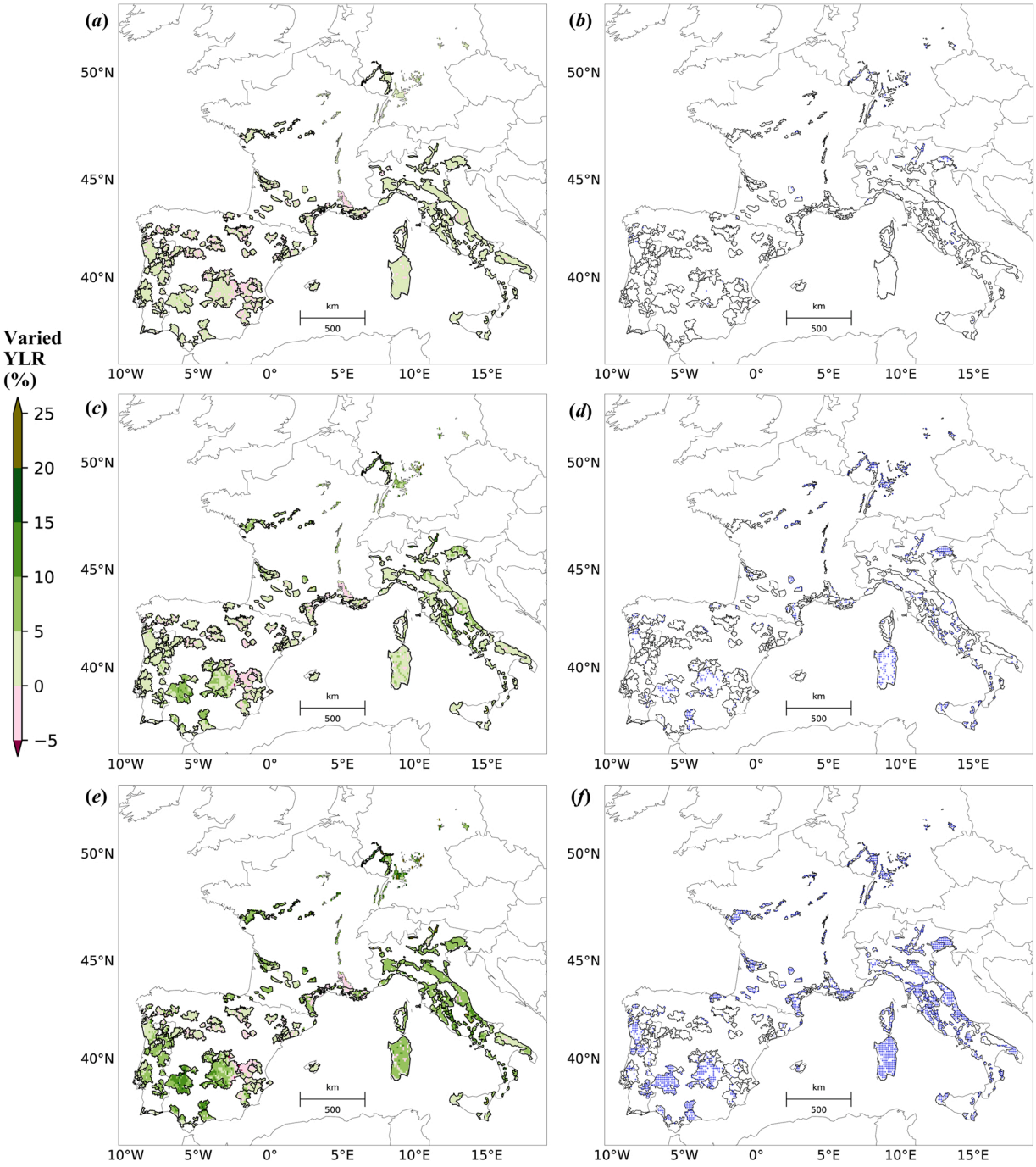

Fig. 6. The median of the variations of the potential yield loss rate (YLR, %) due to seasonal cumulative water stress by shifting the flowering-veraison phase (***a, b***): 5% earlier, (***c, d***): 15% earlier and (***e, f***): 25% earlier. In the right panels, the Mann-Whitney rank test is performed to check if median YLR over 1986—2015 becomes significantly different at $p < =0.05$ (see Section 2.4.4). Significant grids are marked with the blue plus symbol, whereas grids without colours indicate no significance (empty areas). For each grid point, the variations of YLR over 1986—2015 are calculated as the difference (different water-limited potential yields, Section 2.4.4) without and with the shifted phenophase (positive values for reductions on YLR).

parameters that are induced by anticipated higher temperatures. Consequently, the effects of flowering-veraison water deficits on grapevine quality parameters will be dependent on the locations (Ramos and Martínez de Toda, 2020) and the varieties.

3.4.3. Variations of potential YLR

Advanced phenophase seems to result in widespread reductions (alleviations) in potential YLR throughout all studied wine regions (Fig. 6). Reductions of statistical significance are simulated for 15% and 25% shifted phenophase, hence this indicates positive effects on water-limited potential yield (see Section 2.4.4). For I-P-S countries (especially for the drought-prone regions), the median reductions on YLR are generally moderate (<15%), i.e. moderate increase of water-limited potential yields (Fig. 6). It is also accompanied by considerable inter-annual variability, where the 90% uncertainty range is between –20% and 40% (Fig. S13). For F-G-L countries, significant median reductions of YLR, mainly correspond to 5–20% under 15% and 25% shifted phenophase (Fig. 6**c–f**). The respective upper 95th percentile indicates YLR can be potentially reduced by up to 80% (e.g. in Germany) (Fig. S13). Lastly, a linear (negative) relationship is found between CWSI and water-limited potential yield both without and with shifted phenophase (Fig. S14). Clearly, this relationship depends on the year and annual climate conditions (Fig. S14). Yet, it is consistently found shifted phenophase can lead to increased yield sensitivities to drought stress, which is evidenced by increased slope values of linear regressions: without and with 25% shifted phenophase, the estimated potential cluster weight (yield) reductions, as per 0.1 increase in CWSI, are 29–49 g and 33–59 g (90% uncertainty range over 1986–2015) respectively (Fig. S14).

These results suggest advanced phenology tends to have positive effects for water-limited potential yield for most wine regions, which are more effective with 25% shifted phenophase. The flowering-verasion phase represents a crucial period for yield responses to water stress, which has been observed in the fields (Chacón-Vozmediano et al., 2020; Ramos and Martínez-Casasnovas, 2014) and successfully reflected in our simulations (Fig. S14). Gaudin et al. (2014) explicitly report the negative linear relationship between flowering-veraison water stress and berry weight. For I-P-S countries (especially for drought-prone regions), the overall moderate increase of water-limited potential yield, can be associated with the shifted phenophase towards a wetter and cooler period, leading to small but significantly reduced CWSI (Fig. 5**e–f**). These beneficial effects can outweigh the negative impacts on potential yield associated with reduced growth season length, i.e. early ripening and maturity with advanced phenophase. However, for F-G-L countries, increases of water-limited potential yield, can be mainly owing to the shifted growing phase (not only flowering-veraison period) towards a cooler climate with reduced evaporative demand along the season. This can partly offset the adverse effects on yield due to reduced growing length and flowering-veraison precipitation (Fig. S8). It is also because water stress is overall less pronounced in these wine regions (Fig. 4), thus reduced precipitation with advanced phenology has less influence. In addition, for these regions, such as Bordeaux, Moselle, Rheinhessen, advanced phenophase can help avoid crop exposure to possible heat-wave peaks during the ripening period (Fraga et al., 2020). Despite generally potential yield gains with shifted phenophase, drought sensitivities are increased. This is possibly attributed to a shorter growing season with less time for photosynthesis and biomass accumulation, where plant growth and yield formation becomes more sensitive and vulnerable to water stress (van Ittersum et al., 2013). On the other hand, the linear relationship between CWSI and water-limited potential yield is shown to vary with annual climate conditions. It can also depend on genotypic characteristics (Gaudin et al., 2014; Ramos and Martínez-Casasnovas, 2014), which should be further distinguished in subsequent studies.

4. Conclusion

The present study essentially is a retrospective analysis for important wine regions in six different European countries over 1986–2015. The analysis focuses on estimating the mean Crop Water Stress Indicator (CWSI) during a drought-sensitive (flowering-veraison) period (CWSI for brevity) and potential Yield Loss Rate (YLR) (yield refers to cluster weight) resulting from cumulative seasonal water stress. Our findings suggest wine regions prone to a high drought risk (CWSI>0.75) are identified as those in Iberian Peninsula (except north-western Portugal), southern Italy (Apulia, Sardinia, Sicily) and southern France (Languedoc, Provence, Rhone). The corresponding YLR can range from 30% to 60%. In general, wine regions with stronger CWSI during flowering-veraison phase tend to have higher YLR. However, contrasting patterns are found between wine regions in France-Germany-Luxembourg and Italy-Portugal-Spain, which highlights the spatial complexity and contextual-dependent nature for viticulture. In the former case, the test of advanced flowering-veraison phase suggests advanced phenology could have benefited from cooler temperatures and a higher fraction of spring precipitation, resulting in alleviated CWSI with moderate reductions of YLR. Conversely, this may result in decreased flowering-veraison precipitation with more uncertain effects on CWSI in those of France-Germany-Luxembourg. However, since water stress in these regions is generally less severe than those in southern Mediterranean Europe, the shifted phenology towards a cooler season might also lead to increased potential yields (i.e. reduced YLR in extreme years). Nevertheless, effects of shifted phenophase are subject to uncertainties across all wine regions, which might be associated with the strong inter-annual variability of local precipitation.

Overall, we demonstrate the flowering-verasion water availability can be critical to potential vineyard productivity, which is dependent on local soil and climate conditions and genoptyic characteristics. With global warming, such phenophase is expected to be advanced, the obtained positive effects on water stress (reductions) and potential yields under past conditions, depending on the magnitude of warming, can be reversed for local vineyards. Such a trade-off due to interactions between shifting a drought-sensitive phase into a relatively cooler and wetter growing season and changes in local temperature and precipitation patterns, should be explicitly considered in climate impact assessment studies. On the other hand, the underlying implications on grapevine quality parameters are more complex and should be further examined. Such a retrospective analysis might provide new insights towards better management of seasonal water deficit for conventionally vulnerable Mediterranean wine regions, but also for relatively cooler and wetter Central European regions where water stress is becoming increasingly important.

Declaration of Competing Interest

The authors declare that they have no known competing financial interests or personal relationships that could have appeared to influence the work reported in this paper.

Acknowledgments

This study was funded by Clim4Vitis project—“Climate change impact mitigation for European viticulture: knowledge transfer for an integrated approach”, funded by the European Union’s Horizon 2020 Research and Innovation Programme, under grant agreement no. 810176; it was also supported by FCT—Portuguese Foundation for Science and Technology, under the project UIDB/04033/2020. We acknowledge the data provisions from members of the PEP725 project, from IPHEN project and from the Consejo Regulador of Ribera de Duero and Rioja DOCa.

Appendix A. Supporting information

Supplementary data associated with this article can be found in the online version at doi:10.1016/j.agwat.2021.107349.

References

Brisson, N., Itier, B., L'Hotel, J.C., Lorendeau, J.Y., 1998. Parameterisation of the Shuttleworth-Wallace model to estimate daily maximum transpiration for use in crop models. Ecol. Modell. 107, 159–169. https://doi.org/10.1016/S0304-3800(97)00215-9.

FAO/IIASA/ISRIC/ISSCAS/JRC, 2012. Harmonized World Soil Database (version 1.2). FAO, Rome, Italy and IIASA, Laxenburg, Austria.

Allen, R.G., Pereira, L.S., Raes, D., Smith, M., 1998. Crop evapotranspiration - Guidelines for computing crop water requirements - FAO Irrigation and drainage paper 56. Roma.

Angulo, C., Rötter, R., Lock, R., Enders, A., Fronzek, S., Ewert, F., 2013. Implication of crop model calibration strategies for assessing regional impacts of climate change in Europe. Agric. Meteorol. 170, 32–46. https://doi.org/10.1016/j.agrformet.2012.11.017.

OIV, 2021. State of the Vitiviniculture World Market. ⟨https://www.oiv.int/en/technical-standards-and-documents/statistical-analysis/state-of-vitiviniculture⟩. Accessed on 2021–06-01.

Bellvert, J., Marsal, J., Girona, J., Zarco-Tejada, P.J., 2015. Seasonal evolution of crop water stress index in grapevine varieties determined with high-resolution remote sensing thermal imagery. Irrig. Sci. 33, 81–93. https://doi.org/10.1007/s00271-014-0456-y.

Bidabe, B., 1965. L'action des températures sur l'évolution des bourgeons de l'entrée en dormance à la floraison. Congrès Pomologique 51–56.

Brisson, N., Perrier, A., 1991. A semiempirical model of bare soil evaporation for crop simulation models. Water Resour. Res. 27, 719–727. https://doi.org/10.1029/91WR00075.

Brisson, N., Gary, C., Justes, E., Roche, R., Mary, B., Ripoche, D., Zimmer, D., Sierra, J., Bertuzzi, P., Burger, P., Bussière, F., Cabidoche, Y.M., Cellier, P., Debaeke, P., Gaudillère, J.P., Hénault, C., Maraux, F., Seguin, B., Sinoquet, H., 2003. An overview of the crop model stics. Eur. J. Agron. 18, 309–332. https://doi.org/10.1016/S1161-0301(02)00110-7.

Brisson, N., Launay, M., Mary, B., Beaudoin, N., 2009. Conceptual basis, formalisations and parameterization of the STICS crop model. Editions Quae, Versailles, France.

Ceglar, A., van der Wijngaart, R., de Wit, A., Lecerf, R., Boogaard, H., Seguini, L., van den Berg, M., Toreti, A., Zampieri, M., Fumagalli, D., Baruth, B., 2019. Improving WOFOST model to simulate winter wheat phenology in Europe: evaluation and effects on yield. Agric. Syst. 168, 168–180. https://doi.org/10.1016/j.agsy.2018.05.002.

Chacón-Vozmediano, J.L., Martínez-Gascueña, J., García-Navarro, F.J., Jiménez-Ballesta, R., 2020. Effects of Water Stress on Vegetative Growth and 'Merlot' Grapevine Yield in a Semi-Arid Mediterranean Climate. Hortic 6, 95. https://doi.org/10.3390/horticulturae6040095.

Cornes, R.C., van der Schrier, G., van den Besselaar, E.J.M., Jones, P.D., 2018. An Ensemble Version of the E-OBS Temperature and Precipitation Data Sets. J. Geophys. Res. Atmos. 123, 9391–9409. https://doi.org/10.1029/2017JD028200.

Costa, J.M., Vaz, M., Escalona, J., Egipto, R., Lopes, C., Medrano, H., Chaves, M.M., 2016. Modern viticulture in southern Europe: vulnerabilities and strategies for adaptation to water scarcity. Agric. Water Manag 164, 5–18. https://doi.org/10.1016/j.agwat.2015.08.021.

Coucheney, E., Buis, S., Launay, M., Constantin, J., Mary, B., García de Cortázar-Atauri, I., Ripoche, D., Beaudoin, N., Ruget, F., Andrianarisoa, K.S., Le Bas, C., Justes, E., Léonard, J., 2015. Accuracy, robustness and behavior of the STICS soil–crop model for plant, water and nitrogen outputs: evaluation over a wide range of agro-environmental conditions in France. Environ. Model. Softw. 64, 177–190. https://doi.org/10.1016/j.envsoft.2014.11.024.

Fraga, H., Costa, R., Moutinho-Pereira, J., Correia, C.M., Dinis, L.T., Gonçalves, I., Silvestre, J., Eiras-Dias, J., Malheiro, A.C., Santos, J.A., 2015. Modeling phenology, water status, and yield components of three Portuguese grapevines using the STICS crop model. Am. J. Enol. Vitic. 66, 482–491. https://doi.org/10.5344/ajev.2015.15031.

Fraga, H., García de Cortázar Atauri, I., Malheiro, A.C., Santos, J.A., 2016. Modelling climate change impacts on viticultural yield, phenology and stress conditions in Europe. Glob. Chang. Biol. 22, 3774–3788. https://doi.org/10.1111/gcb.13382.

Fraga, H., Molitor, D., Leolini, L., Santos, J.A., 2020. What Is the Impact of Heatwaves on European Viticulture? A Modelling Assessment. Appl. Sci. 10, 3030 https://doi.org/10.3390/app10093030.

Gambetta, G.A., Herrera, J.C., Dayer, S., Feng, Q., Hochberg, U., Castellarin, S.D., 2020. The physiology of drought stress in grapevine: towards an integrative definition of drought tolerance. J. Exp. Bot. 71, 4658–4676. https://doi.org/10.1093/jxb/eraa245.

García de Cortázar-Atauri, I., Brisson, N., Gaudillere, J.P., 2009a. Performance of several models for predicting budburst date of grapevine (Vitis vinifera L.). Int. J. Biometeorol. 53, 317–326. https://doi.org/10.1007/s00484-009-0217-4.

García de Cortázar-Atauri, I., Brisson, N., Ollat, N., Jacquet, O., Payan, J.C., 2009b. Asynchronous dynamics of grapevine (Vitis vinifera) maturation: experimental study for a modelling approach. J. Int. Sci. Vigne Vin. 43, 83–97. https://doi.org/10.20870/oeno-one.2009.43.2.801.

García-Estévez, I., Pérez-Gregorio, R., Soares, S., Mateus, N., de Freitas, V., 2017. Oenological perspective of red wine astringency. OENO One 51. https://doi.org/10.20870/oeno-one.2017.51.2.1816.

Gaudin, R., Kansou, K., Payan, J.-C., Pellegrino, A., Gary, C., 2014. A water stress index based on water balance modelling for discrimination of grapevine quality and yield. J. Int. Sci. Vigne Vin. 48, 1–9. https://doi.org/10.20870/oeno-one.2014.48.1.1655.

Giorgi, F., Lionello, P., 2008. Climate change projections for the Mediterranean region. Glob. Planet. Change 63, 90–104. https://doi.org/10.1016/j.gloplacha.2007.09.005.

Goudriaan, J., van Roermund, H.J.W., 1993. Modelling of ageing, development, delays and dispersion. In: Leffelaar, P.A. (Ed.), On Systems Analysis and Simulation of Ecological Processes with Examples in CSMP and FORTRAN. Springer Netherlands, Dordrecht, pp. 89–126. https://doi.org/10.1007/978-94-011-2086-9_8.

Idso, S.B., Jackson, R.D., Pinter, P.J., Reginato, R.J., Hatfield, J.L., 1981. Normalizing the stress-degree-day parameter for environmental variability. Agric. Meteorol. 24, 45–55. https://doi.org/10.1016/0002-1571(81)90032-7.

García de Cortázar-Atauri, I., 2006. Adaptation du Modèle STICS à la Vigne (Vitis vinifera L.). Utilisation dans le Cadre d'une Étude d'Impact du Changement Climatique à l'Échelle de la France. PhD thesis L'ECOLE NATIONALE SUPERIEURE AGRONOMIQUE DE Montp.

Jackson, R.D., 1982. Canopy Temperature and Crop Water Stress, in: HILLEL, D.B.T.-A. in I. (Ed.). Elsevier, pp. 43–85. https://doi.org/10.1016/B978-0-12-024301-3.50009-5.

Leolini, L., Bregaglio, S., Moriondo, M., Ramos, M.C., Bindi, M., Ginaldi, F., 2018a. A model library to simulate grapevine growth and development: software implementation, sensitivity analysis and field level application. Eur. J. Agron. 99, 92–105. https://doi.org/10.1016/j.eja.2018.06.006.

Leolini, L., Moriondo, M., Fila, G., Costafreda-Aumedes, S., Ferrise, R., Bindi, M., 2018b. Late spring frost impacts on future grapevine distribution in Europe. F. Crop. Res 222, 197–208. https://doi.org/10.1016/j.fcr.2017.11.018.

Mann, H.B., Whitney, D.R., 1947. On a test of whether one of two Random variables is stochastically larger than the other. Ann. Math. Stat. 18, 50–60.

Mariani, L., Alilla, R., Cola, G., Monte, G.D., Epifani, C., Puppi, G., Osvaldo, F., 2013. IPHEN—a real-time network for phenological monitoring and modelling in Italy. Int. J. Biometeorol. 57, 881–893. https://doi.org/10.1007/s00484-012-0615-x.

Molitor, D., Fraga, H., Junk, J., 2020. UniPhen – a unified high resolution model approach to simulate the phenological development of a broad range of grape cultivars as well as a potential new bioclimatic indicator. Agric. . Meteorol. 291, 108024 https://doi.org/10.1016/j.agrformet.2020.108024.

Muñoz Sabater, J., 2019. ERA5-Land hourly data from 1981 to present (Accessed on 01-03-2021). Copernic. Clim. Change Serv. (C3S) Clim. Data Store (CDS). https://doi.org/10.24381/cds.e2161bac.

Parker, A., de Cortázar-Atauri, I.G., Chuine, I., Barbeau, G., Bois, B., Boursiquot, J.-M., Cahurel, J.-Y., Claverie, M., Dufourcq, T., Gény, L., Guimberteau, G., Hofmann, R. W., Jacquet, O., Lacombe, T., Monamy, C., Ojeda, H., Panigai, L., Payan, J.-C., Lovelle, B.R., Rouchaud, E., Schneider, C., Spring, J.-L., Storchi, P., Tomasi, D., Trambouze, W., Trought, M., van Leeuwen, C., 2013. Classification of varieties for their timing of flowering and veraison using a modelling approach: a case study for the grapevine species Vitis vinifera L. Agric. Meteorol. 180, 249–264. https://doi.org/10.1016/j.agrformet.2013.06.005.

Ramos, M.C., 2017. Projection of phenology response to climate change in rainfed vineyards in north-east Spain. Agric. . Meteorol. 247, 104–115. https://doi.org/10.1016/j.agrformet.2017.07.022.

Ramos, M.C., Martinez de Toda, F., 2020. Projecting changes in phenology and grape composition of "Tempranillo" and "Grenache" varieties under climate warming in Rioja DOCa. Vitis Geilweilerhof 59, 181–190. https://doi.org/10.5073/vitis.2020.59.181-190.

Ramos, M.C., Martínez de Toda, F., 2020. Variability in the potential effects of climate change on phenology and on grape composition of Tempranillo in three zones of the Rioja DOCa (Spain). Eur. J. Agron. 115, 126014 https://doi.org/10.1016/j.eja.2020.126014.

Ramos, M.C., Martínez-Casasnovas, J.A., 2014. Soil water variability and its influence on transpirable soil water fraction with two grape varieties under different rainfall regimes. Agric. Ecosyst. Environ. 185, 253–262. https://doi.org/10.1016/j.agee.2013.12.025.

Ramos, M.C., Jones, G.V., Yuste, J., 2015. Spatial and temporal variability of cv. Tempranillo phenology and grape quality within the Ribera del Duero DO (Spain) and relationships with climate. Int. J. Biometeorol. 59, 1849–1860. https://doi.org/10.1007/s00484-015-0992-z.

Ramos, M.C., Pérez-Álvarez, E.P., Peregrina, F., Martínez de Toda, F., 2020. Relationships between grape composition of Tempranillo variety and available soil water and water stress under different weather conditions. Sci. Hortic. (Amst.) 262, 109063. https://doi.org/10.1016/j.scienta.2019.109063.

Richardson, E.A., Seeley, S.D., Walker, D.R., 1974. A model for estimating the completation of rest for "Redhaven" and "Elberta" peach trees. HortScience 9, 331–332.

Rötter, R.P., Hoffmann, M.P., Koch, M., Müller, C., 2018. Progress in modelling agricultural impacts of and adaptations to climate change. Curr. Opin. Plant Biol. 45, 255–261. https://doi.org/10.1016/j.pbi.2018.05.009.

Santos, J.A., Fraga, H., Malheiro, A.C., Moutinho-Pereira, J., Dinis, L.T., Correia, C., Moriondo, M., Leolini, L., Dibari, C., Costafreda-Aumedes, S., Kartschall, T., Menz, C., Molitor, D., Junk, J., Beyer, M., Schultz, H.R., 2020. A review of the potential climate change impacts and adaptation options for European viticulture. Appl. Sci. 10, 3092 https://doi.org/10.3390/app10093092.

Schäfer, J., Friedel, M., Molitor, D., Stoll, M., 2021. Semi-Minimal-Pruned Hedge (SMPH) as a Climate Change Adaptation Strategy: Impact of Different Yield Regulation Approaches on Vegetative and Generative Development, Maturity Progress and

Grape Quality in Riesling. Appl. Sci. 11, 3304 https://doi.org/10.3390/app11083304.
Schultz, H.R., Jones, G.V., 2010. Climate induced historic and future changes in viticulture. J. Wine Res. https://doi.org/10.1080/09571264.2010.530098.
Seidel, S.J., Palosuo, T., Thorburn, P., Wallach, D., 2018. Towards improved calibration of crop models – Where are we now and where should we go? Eur. J. Agron. 94, 25–35. https://doi.org/10.1016/j.eja.2018.01.006.
Shuttleworth, W.J., Wallace, J.S., 1985. Evaporation from sparse crops-an energy combination theory. Q. J. R. Meteorol. Soc. 111, 839–855. https://doi.org/10.1002/qj.49711146910.
Stock, M., Badeck, F., Gerstengarbe, F.-W., Hoppmann, D., Kartschall, T., Österle, H., Werner, P.C., Wodinski, M., 2007. PERSPEKTIVEN DER KLIMAÄNDERUNG BIS 2050 FÜR DEN WEINBAU IN DEUTSCHLAND (KLIMA 2050) (No. 106). Geisenheim.
Templ, B., Koch, E., Bolmgren, K., Ungersböck, M., Paul, A., Scheifinger, H., Rutishauser, T., Busto, M., Chmielewski, F.-M., Hájková, L., Hodzić, S., Kaspar, F., Pietragalla, B., Romero-Fresneda, R., Tolvanen, A., Vučetič, V., Zimmermann, K., Zust, A., 2018. Pan European Phenological database (PEP725): a single point of access for European data. Int. J. Biometeorol. 62, 1109–1113. https://doi.org/10.1007/s00484-018-1512-8.
Tóth, B., Weynants, M., Pásztor, L., Hengl, T., 2017. 3D soil hydraulic database of Europe at 250 m resolution. Hydrol. Process. 31, 2662–2666. https://doi.org/10.1002/hyp.11203.
Valdés-Gómez, H., Celette, F., García de Cortázar-Atauri, I., Jara-Rojas, F., Ortega-Farías, S., Gary, C., 2009. Modelling soil water content and grapevine growth and development with the stics crop-soil model under two different water management strategies. J. Int. Sci. Vigne Vin. 43, 13–28. https://doi.org/10.20870/oeno-one.2009.43.1.806.
van Ittersum, M.K., Cassman, K.G., Grassini, P., Wolf, J., Tittonell, P., Hochman, Z., 2013. Yield gap analysis with local to global relevance—a review. F. Crop. Res. 143, 4–17. https://doi.org/10.1016/j.fcr.2012.09.009.
van Leeuwen, C., Seguin, G., 2006. The concept of terroir in viticulture. J. Wine Res. 17, 1–10. https://doi.org/10.1080/09571260600633135.
van Leeuwen, C., Trégoat, O., Choné, X., Bois, B., Pernet, D., Gaudillère, J.-P., 2009. Vine water status is a key factor in grape ripening and vintage quality for red Bordeaux wine. How can it be assessed for vineyard management purposes? J. Int. Sci. Vigne Vin. 43, 121–134. https://doi.org/10.20870/oeno-one.2009.43.3.798.
van Leeuwen, C., Roby, J.-P., de Rességuier, L., 2018. Soil-related terroir factors: a review. J. Int. Sci. Vigne Vin. 52, 173–188. https://doi.org/10.20870/oeno-one.2018.52.2.2208.
van Leeuwen, C., Destrac-Irvine, A., Dubernet, M., Duchêne, E., Gowdy, M., Marguerit, E., Pieri, P., Parker, A., de Rességuier, L., Ollat, N., 2019. An Update on the Impact of Climate Change in Viticulture and Potential Adaptations. Agron 9, 514. https://doi.org/10.3390/agronomy9090514.
Wallach, D., Buis, S., Lecharpentier, P., Bourges, J., Clastre, P., Launay, M., Bergez, J.-E., Guerif, M., Soudais, J., Justes, E., 2011. A package of parameter estimation methods and implementation for the STICS crop-soil model. Environ. Model. Softw. 26, 386–394. https://doi.org/10.1016/j.envsoft.2010.09.004.
Wenter, A., Zanotelli, D., Montagnani, L., Tagliavini, M., Andreotti, C., 2018. Effect of different timings and intensities of water stress on yield and berry composition of grapevine (cv. Sauvignon blanc) in a mountain environment. Sci. Hortic. (Amst.) 236, 137–145. https://doi.org/10.1016/j.scienta.2018.03.037.
Wu, H., Xiong, D., Liu, B., Zhang, S., Yuan, Y., Fang, Y., Chidi, C.L., Dahal, N.M., 2019. Spatio-Temporal Analysis of Drought Variability Using CWSI in the Koshi River Basin (KRB). Int. J. Environ. Res. Public Heal. https://doi.org/10.3390/ijerph16173100.
Yang, C., Fraga, H., Van Ieperen, W., Santos, J.A., 2018. Modelling climate change impacts on early and late harvest grassland systems in Portugal. Crop Pasture Sci. 69, 821–836. https://doi.org/10.1071/CP17428.
Yang, C., Fraga, H., van Ieperen, W., Santos, J.A., 2020. Assessing the impacts of recent-past climatic constraints on potential wheat yield and adaptation options under Mediterranean climate in southern Portugal. Agric. Syst. 182, 102844 https://doi.org/10.1016/j.agsy.2020.102844.
Yang, C., Menz, C., Fraga, H., Reis, S., Machado, N., Malheiro, A.C., Santos, J.A., 2021. Simultaneous Calibration of Grapevine Phenology and Yield with a Soil–Plant–Atmosphere System Model Using the Frequentist Method. Agron 11, 1659. https://doi.org/10.3390/agronomy11081659.
Zheng, W., del Galdo, V., García, J., Balda, P., Martínez de Toda, F., 2017. Use of minimal pruning to delay fruit maturity and improve berry composition under climate change, 136 LP – 140 Am. J. Enol. Vitic. 68, 136–140. https://doi.org/10.5344/ajev.2016.16038.
Zhu, X., Xu, K., Liu, Y., Guo, R., Chen, L., 2021. Assessing the vulnerability and risk of maize to drought in China based on the AquaCrop model. Agric. Syst. 189, 103040 https://doi.org/10.1016/j.agsy.2020.103040.